The Journal of Neuroscience, June 1, 2001, *21*(11):3721–3728

Presynaptic Ca^{2+} Channels and Neurotransmitter Release at the Terminal of a Mouse Cortical Neuron

Jing Qian and Jeffrey L. Noebels

Department of Neurology, Baylor College of Medicine, Houston, Texas 77030

Regional variation in synaptic efficacy is an important determinant of associative processing as information flows through major circuits of the brain. The perforant path is the principal route of entry from cortex to the hippocampus and contains the first synapse in the cortical–hippocampal projection pathway. We used optical imaging techniques to analyze presynaptic Ca^{2+} entry and neurotransmitter release at synapses in the medial perforant path linking stellate neurons located in layer II of the entorhinal cortex to granule cells in the dentate gyrus. Similar to other excitatory central synapses, the relationship between neurotransmitter release and the amount of Ca^{2+} influx can be best described by a Hill equation with a Hill coefficient of 3.5. Our Ca^{2+} channel toxin studies indicate that P/Q-type channels are the predominant Ca^{2+} source triggering neurotransmitter release in this pathway, as shown by a potent inhibition of Ca^{2+} entry and synaptic transmission by the P/Q-type channel blocker ω-agatoxin IVA. However, compared with the downstream hippocampal pyramidal neuron CA3–CA1 synapse, neurotransmitter release was less sensitive to the N-type Ca^{2+} channel blocker ω-conotoxin GVIA, although the amount of N-type Ca^{2+} current is comparable. The contribution of N-type channels to neurotransmitter release approximates that found at the CA3–CA1 synapse when tested under lower $[Ca^{2+}]_o$, which effectively reduces the size of the Ca^{2+} microdomain surrounding each channel. These results suggest that P/Q-type channels are more closely associated with release machinery then N-type channels at this synapse and that cooperativity differences for each channel subtype may characterize variations in signaling at central synapses.

Key words: presynaptic calcium entry; corticohippocampal synapse; medial perforant path; synaptic efficacy; power relationship; cooperativity; optical imaging.

Synaptic efficacy is a critical determinant of functional connectivity and plasticity within central neural networks and may vary throughout development from zero ("silent synapses") to an optimal value for signaling. Recent study of synaptic transmission between cortical neurons indicates that different types of neurons release neurotransmitter with different degrees of efficacy. Reliable quantal release of neurotransmitter with a few failures was found at the synaptic connection between spiny stellate cells in layer IV of rat somatosensory cortex, in contrast to the low release probability observed at synapses between pyramidal cells in layer V (Feldmeyer et al., 1999; Feldmeyer and Sakmann, 2000). Although excitation–release coupling at terminals involves a complex series of events, from the standpoint of Ca^{2+} ion entry, the probability of release is dependent on the type and density of presynaptic Ca^{2+} channels expressed and their individual proximity to and interaction with transmitter release machinery. Because of the limitation of current electrophysiological techniques, it has been difficult to directly access presynaptic Ca^{2+} currents to determine the mechanism for the distinct release probabilities at these synapses and the role of specific calcium channel subtypes at terminals of cortical neurons.

One major subcortical pathway that originates from cortical stellate neurons is the synaptic projection from the entorhinal cortex to the hippocampus, the medial perforant pathway. Spiny stellate neurons are the most abundant cell type in layer IV of neocortex and layer II of entorhinal cortex (Woolsey et al., 1975; Feldman and Peters, 1978; Klink and Alonso, 1997). Their functional role is presently thought of as an information amplifier that collects inputs destined to the cortex and then relays this information both to other cortical layers and over longer distances to subcortical brain networks. Spiny stellate neurons located in the layer II of the medial entorhinal cortex extend their axons subcortically to synapse on the dendrites of granule cells within the outer two-thirds of the molecular layer of the dentate gyrus (Steward and Scoville, 1976). Therefore, study of the presynaptic Ca^{2+} currents and synaptic transmission in the hippocampal medial perforant pathway could provide the first insight into the characteristics of presynaptic Ca^{2+} channels and neurotransmitter release of a major cortical projection neuron.

The laminar synaptic organization in the molecular layer of the dentate gyrus offers an anatomical advantage to selectively load and optically isolate a defined population of presynaptic terminals, similar to that found in the stratum radiatum of the hippocampal CA3–CA1 area in which fluorescence Ca^{2+} imaging has been used to access presynaptic Ca^{2+} currents in several species (Wu and Saggau, 1994a; Qian et al., 1997; Qian and Noebels, 2000). In this study, we use the same technique to explore the types of presynaptic Ca^{2+} channels and neurotransmitter release in the mouse medial perforant pathway. Our study identifies a distinct difference in the cooperativity of neurotransmitter release for each Ca^{2+} channel subtype at the presynaptic terminals of cortical stellate neurons compared with the hippocampal CA3–CA1 synapses that lie immediately downstream.

Received Dec. 11, 2000; revised March 13, 2001; accepted March 13, 2001.

This work was supported by an Eric Lothman Postdoctoral Fellowship from the American Epilepsy Society/Milken Foundation (J.Q.) and National Institute of Neurological Disorders and Stroke Grant NS29709 (J.L.N.).

Correspondence should be addressed to Dr. Jeffrey L. Noebels, Department of Neurology, Baylor College of Medicine, One Baylor Plaza, Houston, TX 77030. E-mail: jnoebels@bcm.tmc.edu.

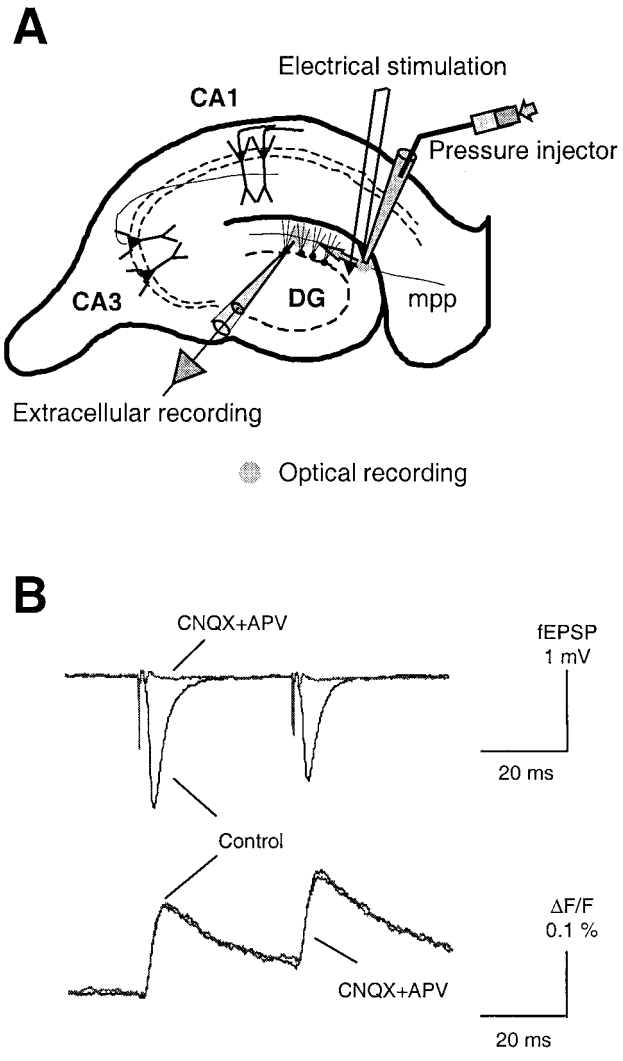

Figure 1. Recording presynaptic Ca^{2+} influx and postsynaptic response in the mouse hippocampal medial perforant pathway. *A*, A schematic diagram for loading Ca^{2+} indicator into presynaptic terminals of the hippocampal medial perforant pathway. *B*, Sample traces of $[Ca_{pre}]_t$ and fEPSP in response to a pair of stimuli.

MATERIALS AND METHODS

Transverse brain slices (315 μm thickness) were prepared from hippocampi of adult wild-type mice (between 4 and 9 months old) and incubated at 25°C in artificial CSF containing (in mM): 124 NaCl, 3.5 KCl, 2.5 $CaCl_2$, 2 $MgCl_2$, 22 $NaHCO_3$, 1.25 NaH_2PO_4, and 10 D-glucose, gassed with 95% O_2–5% CO_2 to maintain a constant pH of 7.4. The slices were transferred into a recording chamber controlled at 30°C for the loading of Ca^{2+} indicator and subsequent fluorescence imaging.

The low-affinity Ca^{2+}-sensitive fluorescence indicator Magnesium Green-AM (Molecular Probes, Eugene, OR) was loaded into presynaptic terminals of the medial perforant pathway by a method similar to that used at the mouse hippocampal CA3–CA1 synapse (Qian and Noebels, 2000). Figure 1 shows a schematic diagram for the loading of Ca^{2+} indicator and the recording of optical and electrophysiological signals. A small amount of dye dissolved in DMSO solution was pressure injected into the middle of the molecular layer of dentate gurus in which axons from the projection neurons located in the layer II of entorhinal cortex terminate and synapse with dendrites of granule cells. A small recording area in the middle of the molecular layer with a diameter of 150 μm was excited at a wavelength of 488 ± 20 nm; the emitted fluorescence was filtered using a bandpass filter of 535 ± 25 nm and converted into an electrical signal with a single photodiode. A bipolar tungsten electrode was positioned in the molecular layer, ~0.5–0.8 mm away from the recording area (as shown in Fig. 1) to stimulate the medial perforant pathway. Stimuli were delivered every 20 sec using current pulses of 0.03–0.05 mA/0.1 msec to elicit a submaximal response. The stimulation-induced presynaptic Ca^{2+} transient ($[Ca_{pre}]_t$) and the evoked field EPSP (fEPSP) were simultaneously sampled at 10 kHz. Three successive traces were averaged to improve the signal-to-noise ratio. The maximal slope of the fEPSP was taken as the measure of synaptic transmission. For field recording, glass microelectrodes (1–5 MΩ, filled with 2 M NaCl) were positioned in the center of the optical recording area. At the beginning of each experiment, a pair of stimulating pulses separated by an interval of 40 msec was given to test for activation of the medial perforant pathway. The response of the medial perforant pathway was judged by the presence of short-term inhibition of synaptic transmission, as shown by the sample trace in Figure 1. Ca^{2+} influx was measured by the fluorescence ratio of $\Delta F/F$. Autofluorescence of the brain slice was subtracted from the total fluorescence signal. The selective presynaptic loading of the Ca^{2+} indicator in the mouse hippocampal slice was verified by applying the glutamate receptor antagonists 6-cyano-7-nitroquinoxaline-2,3-dione (CNQX) (10 μM) and D-amino-phosphonovalerate (D-APV) (25 μM) at the end of each experiment. As shown in Figure 1, the glutamate receptor antagonists did not alter the optical signal, $\Delta F/F$, but completely blocked the fEPSP, indicating a pure presynaptic origin of optical signals. The signal containing the fiber volley and stimulation artifact obtained after application of CNQX and APV was then used as a template to subtract these components from the raw recording trace of fEPSP before measuring the slope of the response. Unless otherwise stated, data in each experiment were normalized to the baseline before any drug application and then pooled together and expressed as mean ± SD.

Drugs. Ca^{2+} channel toxin ω-conotoxin GVIA (ω-CgTx GVIA), ω-agatoxin IVA (ω-Aga IVA), and ω-CgTx MVIIC were purchased from Bachem AG (Bubendorf, Switzerland). CNQX and D-APV purchased from Tocris Cookson (Ballwin, MO).

RESULTS

Presynaptic Ca^{2+} channel types responsible for neurotransmission in the hippocampal medial perforant pathway

The types of Ca^{2+} channels mediating neurotransmitter release at the synaptic connection from entorhinal cortex to hippocampal dentate gyrus were first evaluated by application of selective Ca^{2+} channel toxins. Figure 2*A* shows the time course of $[Ca_{pre}]_t$ and fEPSP from a representative experiment before, during, and after bath perfusion of 1 μM ω-CgTx GVIA, the selective N-type Ca^{2+} channel blocker. As shown in Figure 2*A*, the toxin substantially reduced $[Ca_{pre}]_t$ but had only a minor effect on synaptic transmission. The mean inhibition of $[Ca_{pre}]_t$ and fEPSP by ω-CgTx GVIA was ~31 ± 6 (n = 9) and 12 ± 3% (n = 9), respectively. Although the amount of $[Ca_{pre}]_t$ reduced by the toxin at this synapse was comparable with that measured at the hippocampal CA3–CA1 synapse of the same mouse strain (Qian and Noebels, 2000), a much reduced effect of N-type Ca^{2+} channel blockade on synaptic transmission (12 ± 3 versus 45 ± 4% at the CA3–CA1 synapse) was observed here. The contribution of P/Q-type channels to neurotransmitter release was measured by bath perfusion of 1 μM ω-Aga IVA, the selective P/Q-type Ca^{2+} channel blocker. As revealed by the time course shown in Figure 2*B*, application of the toxin sharply reduced $[Ca_{pre}]_t$ and potently inhibited synaptic transmission. On average, ω-Aga IVA reduced $[Ca_{pre}]_t$ by 53 ± 5% (n = 3) and inhibited the fEPSP by 86 ± 2% (n = 3). These data indicate that, similar to other excitatory central synapses studied to date, Ca^{2+} entering through P/Q-type channels is the major source of Ca^{2+} triggering neurotransmitter release in response to stimulation of the hippocampal medial perforant pathway.

We also measured the $[Ca_{pre}]_t$ and fEPSP after blocking both P/Q- and N-type Ca^{2+} channels to assess the remaining contri-

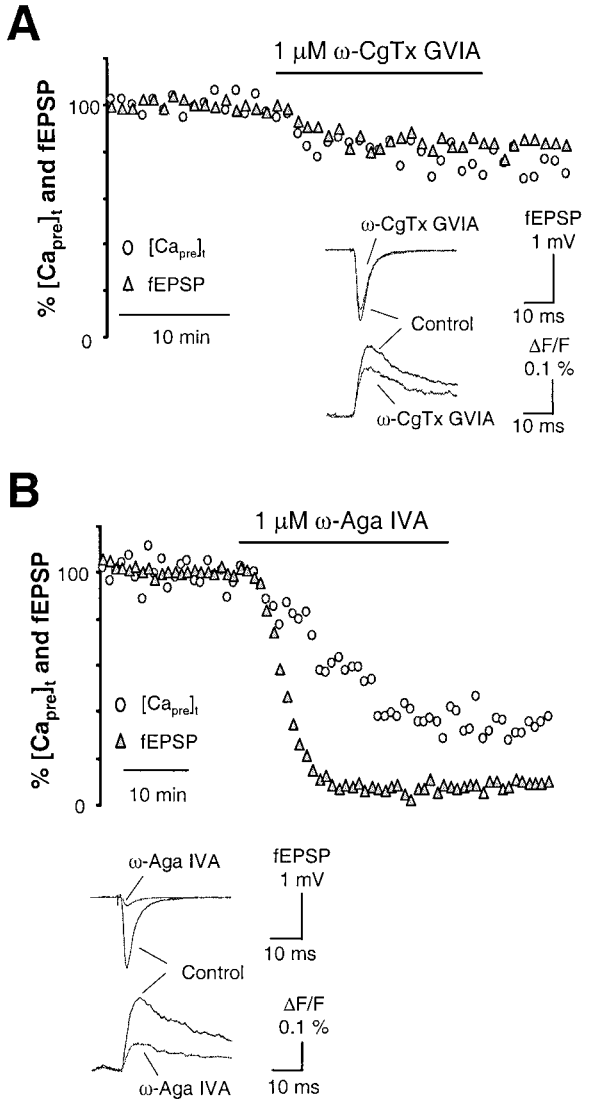

Figure 2. Types of presynaptic Ca^{2+} channels controlling neurotransmitter release in the hippocampal medial perforant pathway. *A*, Time courses of $[Ca_{pre}]_t$ and fEPSP in response to 1 μM ω-CgTx GVIA, the N-type Ca^{2+} channel blocker, in the hippocampal medial perforant pathway. The toxin substantially reduced $[Ca_{pre}]_t$ but had only a minor effect on synaptic transmission. The mean inhibition of $[Ca_{pre}]_t$ and fEPSP by ω-CgTx GVIA was ~31 ± 6 and 12 ± 3% (n = 9). Although the amount of $[Ca_{pre}]_t$ reduced by the toxin at this synapse was comparable with that measured at the hippocampal CA3–CA1 synapse of the same species, much less effect of N-type Ca^{2+} channel blockade on synaptic transmission was observed here. *Inset* shows sample traces taken during steady-state periods in the control solution and after application of ω-CgTx GVIA. *B*, Time courses of $[Ca_{pre}]_t$ and fEPSP in response to 1 μM ω-Aga IVA, the P/Q-type Ca^{2+} channel blocker. Application of the toxin strikingly reduced $[Ca_{pre}]_t$ and potently inhibited synaptic transmission. On average, ω-Aga IVA reduced $[Ca_{pre}]_t$ by 53 ± 5% (n = 3) and inhibited the fEPSP by 86 ± 2% (n = 3). These data indicate that, similar to other excitatory central synapses studied to date, Ca^{2+} entering through P/Q-type channels is the major source of Ca^{2+} triggering release of neurotransmitter in the hippocampal medial perforant pathway. *Inset* shows sample traces taken during steady-state periods in the control solution and after application of ω-Aga IVA.

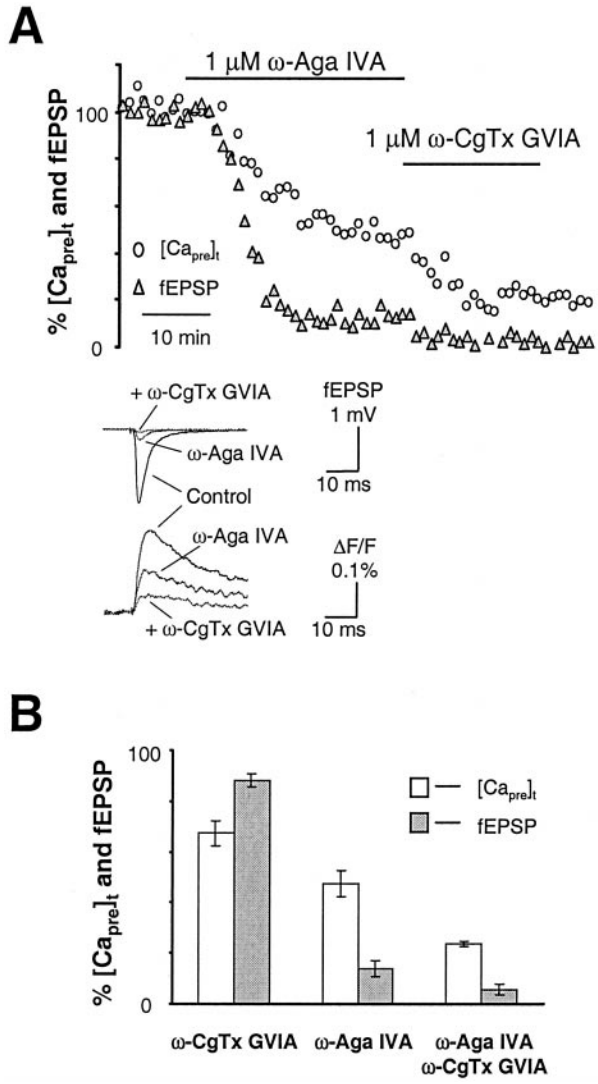

Figure 3. Blocking both P/Q- and N-type channels eliminates the release of neurotransmitter in the hippocampal medial perforant pathway. *A*, Time courses of $[Ca_{pre}]_t$ and fEPSP in response to 1 μM ω-Aga IVA and 1 μM CgTx GVIA together. Combined application of two toxins reduced $[Ca_{pre}]_t$ to 24 ± 1% (n = 2) of baseline and almost completely eliminated synaptic transmission. The average fEPSP was 6 ± 2% of baseline (n = 2). *Inset* shows sample traces taken during steady-state periods in the control solution and after application of ω-Aga IVA and ω-CgTx GVIA. *B*, Summary data comparing the inhibition of $[Ca_{pre}]_t$ and fEPSP in response to application of ω-CgTx GVIA and ω-Aga IVA. P/Q- and N-type channels are the major Ca^{2+} source controlling neurotransmitter release at this synapse.

bution of other Ca^{2+} channel types. Figure 3*A* shows the time course of the $[Ca_{pre}]_t$ and fEPSP during application of ω-CgTx GVIA after previous blockade of P/Q-type channels with ω-Aga IVA. Combined application of both toxins reduced $[Ca_{pre}]_t$ to 24 ± 1% (n = 2) of baseline and almost completely eliminated synaptic transmission. The average fEPSP was 6 ± 2% of baseline (n = 2). The possible involvement of L-type Ca^{2+} channels in the residual release of neurotransmitter at this synapse was also tested. Similar to the findings at other central synapses (Wu and Saggau, 1994b; Mintz et al., 1995; Wu et al., 1999), L-type Ca^{2+} channels did not contribute to Ca^{2+} influx at presynaptic terminals in this pathway, as indicated by the lack of significant effects of the L-type channel antagonist nifedipine (10 μM) on $[Ca_{pre}]_t$ and fEPSP (data not shown). Figure 3*B* summarizes the results obtained from experiments after the application of Ca^{2+} channel toxins.

Ca^{2+} cooperativity of neurotransmitter release through P/Q- and N-type channels in the hippocampal medial perforant pathway

In addition to the types of voltage-dependent Ca^{2+} channels mediating Ca^{2+} entry at the terminal, the relationship between presynaptic Ca^{2+} influx and neurotransmitter release is a second critical aspect characterizing the Ca^{2+} induced-release of neurotransmitter. Previous studies in the CNS show that neurotransmitter release is a power function of presynaptic Ca^{2+} current, with a power number between 3 and 4 (Wu and Saggau, 1994a; Mintz et al., 1995; Borst and Sakmann, 1996). Here, we investigated this power relationship in the hippocampal medial perforant pathway by measuring $[Ca_{pre}]_t$ and fEPSP amplitudes while varying extracellular Ca^{2+} concentration ($[Ca^{2+}]_o$) from 2.5 mM under control conditions up to 4 mM and down to 1.5, 1.0, 0.75, and 0.5 mM, respectively. In each experiment, the extracellular Mg^{2+} level was either reduced to 0.5 mM (in the case of 4 mM $[Ca^{2+}]_o$) or raised appropriately to maintain the size of the presynaptic fiber volley constant. As shown in Figure 4*A*, at the end of each experiment, two glutamate receptor antagonists, CNQX and APV, were routinely applied to isolate the stimulation artifact and presynaptic fiber volley. There were two purposes for this experimental manipulation. One was to allow subtraction of the stimulation artifact and presynaptic fiber volley from the raw recording trace for a more accurate measurement of the fEPSP slope. Another was to determine the presence of any postsynaptic contamination of Ca^{2+} indicator labeling, which would cause an underestimation of the power relationship. As shown by the sample trace in the *inset* of Figure 4*A*, the Ca^{2+} signal measured in our experiments was purely presynaptic, because there was no significant difference between $[Ca_{pre}]_t$ before or after the combined application of CNQX and APV to block the postsynaptic response (the mean difference was $3 \pm 4\%$; $n = 25$). Figure 4*B* summarizes the $[Ca_{pre}]_t$ and fEPSP amplitudes obtained at steady state during reduction of $[Ca^{2+}]_o$ from control levels to a particular test concentration. $[Ca_{pre}]_t$ was 75 ± 7 ($n = 6$), 60 ± 2 ($n = 5$), 50 ± 2 ($n = 5$), and $44 \pm 2\%$ ($n = 2$) of baseline when exposed to 1.5, 1.0, 0.75, and 0.5 mM $[Ca^{2+}]_o$, respectively. The corresponding fEPSPs were 61 ± 7, 34 ± 2, 17 ± 2, and $2 \pm 1\%$ of baseline. To test whether neurotransmitter release was saturated by the amount of Ca^{2+} influx under control conditions, we measured the $[Ca_{pre}]_t$ and fEPSP under 4 mM $[Ca^{2+}]_o$. In these experiments, the average $[Ca_{pre}]_t$ increased to $151 \pm 15\%$ ($n = 7$) of baseline. The corresponding mean fEPSP was $131 \pm 11\%$ ($n = 7$) of baseline, a substantial increase, but much less than what would be obtained if it adhered to the power law. This indicates that, although the basal level of release is not saturated by the amount of Ca^{2+} influx under control conditions, it operates in the upper part of the synaptic transmission curve as shown in Figure 4*B*. The synaptic transmission curve in Figure 4*B* is a best fit of experimental data with the following Hill equation: $fEPSP = fEPSP_{max}[([Ca_{pre}]_t)^n/([Ca_{pre}]_f)^n + (K_d)^n]$, where n is the Hill coefficient and represents the degree of Ca^{2+} cooperativity in the process of release, $fEPSP_{max}$ is the maximal fEPSP (normalized to control), and K_d is the amount of $[Ca_{pre}]_t$ when fEPSP is 50% of the maximal amplitude. At this synapse, the Ca^{2+} cooperativity of neurotransmitter release is $n = 3.5$. This is consistent with findings at other central synapses (Wu and Saggau, 1994a; Mintz et al., 1995; Borst and Sakmann, 1996). To compare the results with those obtained from the CA3–CA1 synapse (Qian and Noebels, 2000), Figure 4*C* shows the calculated apparent power numbers [defined as $\log(fEPSP\%)/\log([Ca_{pre}]_t\%)$], corresponding to each tested $[Ca^{2+}]_o$. Data from experiments using 0.5 mM $[Ca^{2+}]_o$ are not included because the slope of the fEPSP at 0.5 mM $[Ca^{2+}]_o$ was very small and comparable with noise level. The average apparent power numbers were dependent on the tested $[Ca^{2+}]_o$ and were 0.7 ± 0.2 ($n = 7$), 1.7 ± 0.3 ($n = 6$), 2.1 ± 0.1 ($n = 5$), and 2.6 ± 0.3 ($n = 5$) for 4.0, 1.5, 1.0, and 0.75 mM, respectively. We also independently calculated the power relationship for transmission at this synapse while selectively reducing Ca^{2+} entry through a particular type of Ca^{2+} channel. The mean apparent power number obtained during blockade of P/Q channels was 2.7 ± 0.5 ($n = 3$), and the mean apparent power number obtained during N-type blockade was 0.4 ± 0.1 ($n = 9$). The very low power number obtained for N-type channel coupling cannot be simply explained by the dose–response curve of the apparent power number to the $[Ca_{pre}]_t$, because reduction of $[Ca_{pre}]_t$ to 75% of baseline with 1.5 mM $[Ca^{2+}]_o$ produced a greater power number. Rather, the high power number in the relationship between $[Ca_{pre}]_t$ and neurotransmitter release mediated by P/Q-type channels suggests that P/Q channels are more tightly coupled with the vesicle release machinery than N-type channels.

Colocalization of P/Q- and N-type Ca^{2+} channels at the release site in the hippocampal medial perforant pathway

Our measured signal at perforant path synapses onto granule cell dendrites reflects a population response of single corticofugal presynaptic terminals, and their release properties are not necessarily uniform. Application of ω-Aga IVA resulted in ~86% reduction of synaptic transmission, whereas ω-CgTx GVIA reduced synaptic transmission by only 12%. If these values were superadditive (sum in excess of 100%), the results would be taken as evidence for colocalization of P/Q- and N-type channels at the same presynaptic terminals and for an anatomically overlapping contribution of multiple Ca^{2+} channel types in neurotransmitter release (Wheeler et al., 1994; Wu and Saggau, 1994b; Mintz et al., 1995). In the present case, the sum of both values was ~100%. This result can be interpreted as reflecting a segregation of P/Q- and N-type channels at different sets of presynaptic terminals or as indicating that Ca^{2+} microdomains around each channel do not overlap. Alternatively, the lack of superaddition might be coincidental, and the minor effect on neurotransmitter release observed by blocking N-type channels could be attributable to high Ca^{2+} entry near the presynaptic release site.

To distinguish between these two hypotheses, we repeated the Ca^{2+} channel toxin experiments shown in Figure 2 under a condition of low $[Ca^{2+}]_o$ (1.0 mM), which would reduce Ca^{2+} currents and thereby effectively shrink the size of the functional Ca^{2+} microdomain. If P/Q- and N-type Ca^{2+} channels are segregated in different sets of presynaptic terminals or their microdomains are not overlapping, the total reduction should remain at ~100% in 1.0 mM $[Ca^{2+}]_o$. If not, a superaddition in the fractional reduction of neurotransmitter release by selectively blocking P/Q- and N-type channels would be expected. Consistent with the latter hypothesis, as shown by the experiment in Figure 5*A*, the inhibition of synaptic transmission by ω-CgTx-GVIA was increased to $37 \pm 3\%$ ($n = 6$) in 1.0 mM $[Ca^{2+}]_o$. The mean reduction of $[Ca_{pre}]_t$ was $27 \pm 7\%$ ($n = 5$). Figure 5*B* shows a representative experiment with ω-Aga IVA. On average, the toxin reduced neurotransmitter release by $94 \pm 1\%$ ($n = 4$) in 1.0 mM $[Ca^{2+}]_o$. The mean reduction of $[Ca_{pre}]_t$ was $56 \pm 6\%$ ($n = 2$). The sum of reductions in neurotransmitter release by selectively blocking both P/Q- or N-type channels therefore ex-

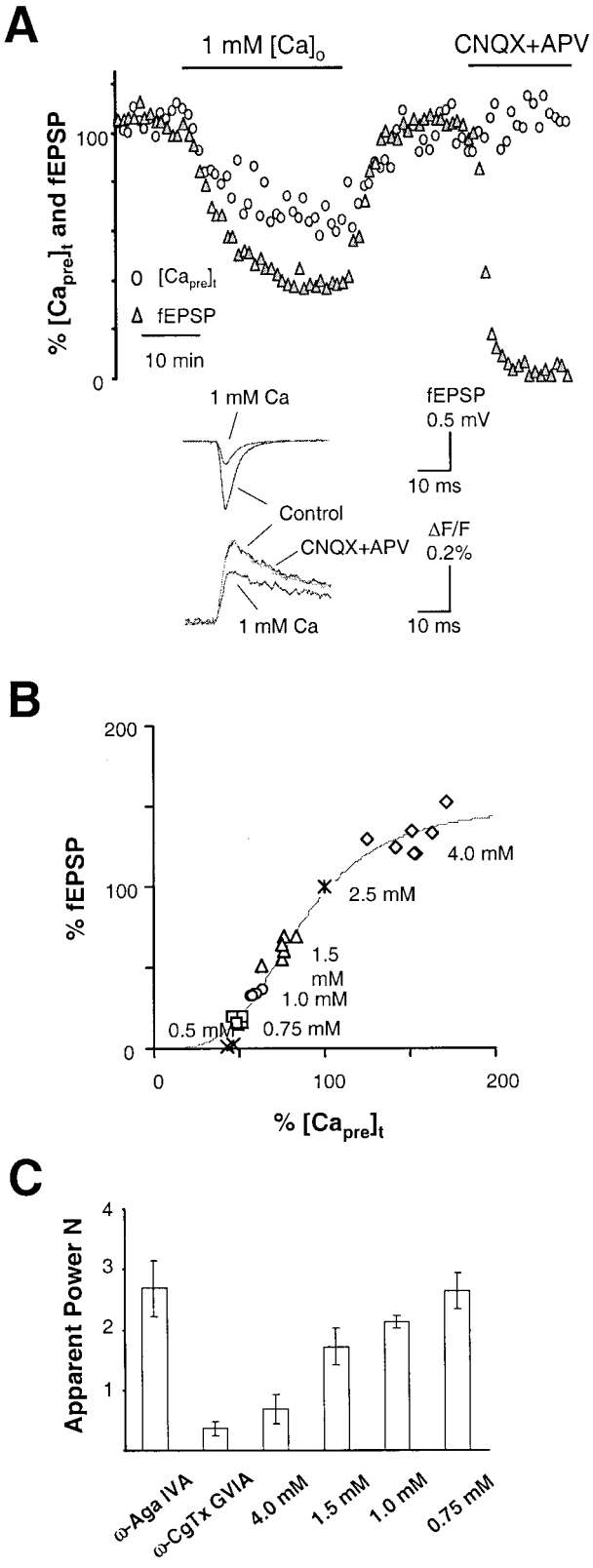

Figure 4. Relationship between Ca^{2+} entry and the release of neurotransmitter in the hippocampal medial perforant pathway. *A*, Time courses of $[Ca_{pre}]_t$ and fEPSP in response to the manipulation of extracellular Ca^{2+} concentration ($[Ca^{2+}]_o$) in a typical experiment. At the end of each experiment, two glutamate receptor antagonists, CNQX and APV, were routinely applied to isolate the stimulation artifact and presynaptic fiber volley. This allows subtraction of the stimulation artifact and presynaptic fiber volley from the raw recording trace for a more accurate measurement of the slope of fEPSP. *Inset* shows sample traces taken at steady state in solutions containing 2.5 mM $[Ca^{2+}]_o$ (control), 1.0 mM $[Ca^{2+}]_o$, and after application of CNQX and APV. *B*, Summary data of $[Ca_{pre}]_t$ and fEPSP in response to each $[Ca^{2+}]_o$ tested. The *solid line* is a best fit of experimental data with a Hill equation: $fEPSP = fEPSP_{max}[([Ca_{pre}]_t)^n/([Ca_{pre}]_t)^n + (K_d)^n]$. $fEPSP_{max} = 150\%$ of baseline fEPSP, and $K_d = 85\%$ of baseline $[Ca_{pre}]_t$; $n = 3.5$. *C*, Comparison of the apparent power number $[\log(\%fEPSP)/\log(\%[Ca_{pre}]_t)]$ as a result of selective blockade of Ca^{2+} channels and nonselective reduction of Ca^{2+} entry. The calculated apparent power numbers for ω-Aga IVA and ω-CgTx GVIA are 2.7 ± 0.5 ($n = 3$) and 0.4 ± 0.1 ($n = 9$), respectively. The calculated apparent power numbers for 4.0, 1.5, 1.0, and 0.75 mM $[Ca^{2+}]_o$ are 0.7 ± 0.2 ($n = 7$), 1.7 ± 0.3 ($n = 6$), 2.1 ± 0.1 ($n = 5$), and 2.6 ± 0.3 ($n = 5$), respectively. This result indicates that P/Q-type channels interact with the release machinery more tightly than N-type in the hippocampal medial perforant pathway.

ceeded 100%. Compared with control saline, the relatively larger reductions of fEPSP in 1.0 mM $[Ca^{2+}]_o$ by these two toxins indicate increased cooperativity of N- and P/Q-type channels in controlling neurotransmitter release when the size of Ca^{2+} microdomains around each channel was reduced. These results clearly indicate that P/Q- and N-type Ca^{2+} channels are colocalized at the release site.

DISCUSSION

The neuroanatomical isolation of presynaptic terminals originating from stellate cells in the entorhinal cortex and terminating in the hippocampal formation facilitates the analysis of release properties at cortical synapses. In this study, we have examined the subtypes of Ca^{2+} channels and their cooperativity in controlling the release of neurotransmitter at a mouse cortical synapse.

Anatomy of the corticohippocampal perforant path projection

Axons from the entorhinal cortex to the dentate gyrus constitute the principal cortical input to the hippocampal formation. Two major divisions, the medial and lateral perforant pathways, project to different regions of the hippocampus. The medial pathway studied here emanates from neurons located in layer II of the medial entorhinal cortex. These axons terminate in a highly restricted band favorable for optical imaging within the midportion of the molecular layer of the dentate gyrus and form synaptic connections with dendrites of granule cells (Steward and Scoville, 1976). Two distinct categories of projection neurons in layer II of the entorhinal cortex have been defined on the basis of their morphology and electrical membrane properties (Steward and Scoville, 1976; Alonso and Klink, 1993). Over two-thirds of these neurons belong to the category of spiny stellate cells (Alonso and Klink, 1993), whereas pyramidal-like neurons are much less abundant and constitute the remainder. In addition to outnumbering pyramidal-like cells, stellate neurons also produce more extensive patterns of recurrent axonal collaterization (Klink and Alonso, 1997). Therefore, the majority of axons terminating in the molecular layer of the dentate gyrus originate from stellate cells located in layer II of the entorhinal cortex. Consistent with this estimate, we observed a short-term depression of synaptic transmission in our experiments when a paired-pulse stimulation was given. This is in close agreement with the behavior of synaptic connections between stellate cells in layer IVA of rat somatosensory cortex, in which a prominent short-term depression of synaptic transmission resulting from high release probabilities at presynaptic terminals of stellate cells was reported (Egger et al., 1999) and with earlier analysis of the perforant pathway (Mc-

←

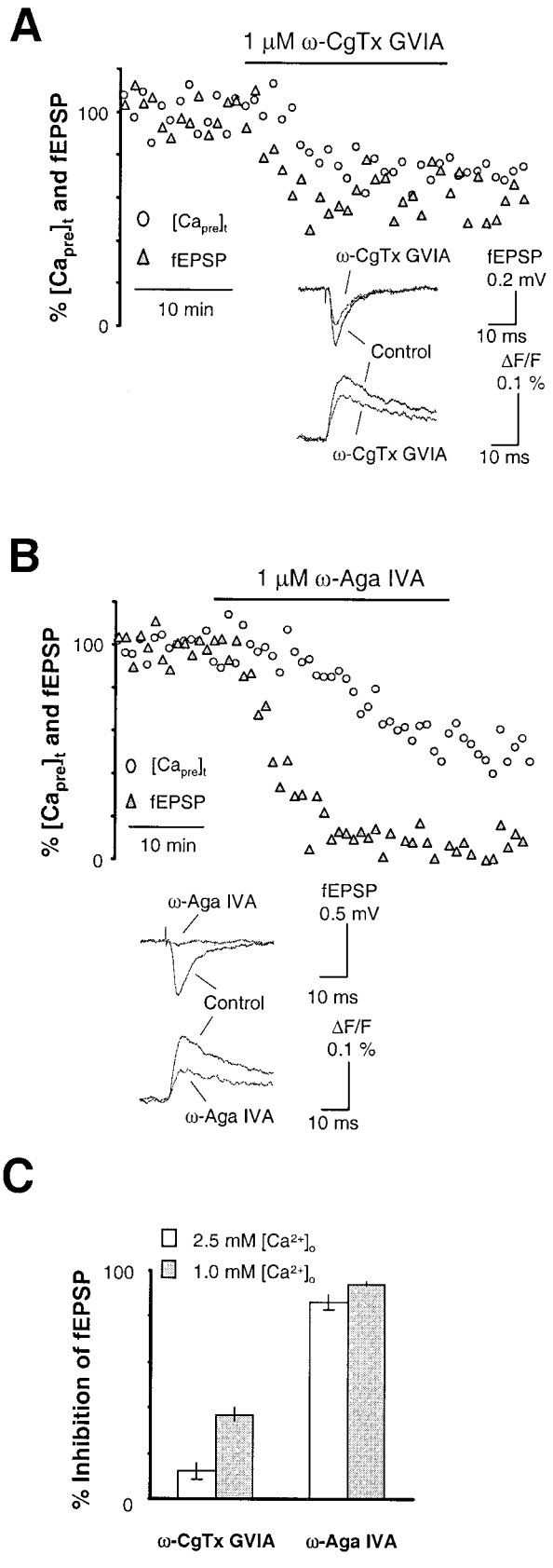

Figure 5. Increased cooperativity of N- and P/Q-type Ca^{2+} channels in controlling neurotransmitter release under lower $[Ca^{2+}]_o$. *A*, *B*, Time course of neurotransmitter release in response to N- and P/Q-type Ca^{2+} channel blockers when tested under lower $[Ca^{2+}]_o$. *Insets* show sample traces of fEPSP and $[Ca_{pre}]_t$ before and after application of ω-CgTx GVIA and ω-Aga IVA under a condition of 1 mM $[Ca^{2+}]_o$. *C*, Summary data for the inhibition of synaptic transmission by 1 μM ω-CgTx GVIA and 1 μM ω-Aga IVA under 1 mM $[Ca^{2+}]_o$. The inhibition of fEPSP by ω-CgTx GVIA was increased from 12 ± 3% (n = 9) under 2.5 mM $[Ca^{2+}]_o$ to 37 ± 3% (n = 5) under 1.0 mM $[Ca^{2+}]_o$. Meanwhile, the inhibition of synaptic transmission by ω-Aga IVA increased from 86 ± 2% (n = 3) under 2.5 mM $[Ca^{2+}]_o$ to 94 ± 1% (n = 4) under 1.0 mM $[Ca^{2+}]_o$. These results are consistent with the hypothesis that P/Q- and N-type Ca^{2+} channels are colocalized at the release site, and the insensitivity of neurotransmitter release to ω-CgTx GVIA under control conditions is attributable in part to high Ca^{2+} entry at this synapse.

Naughton, 1980). Thus, our fluorescence imaging and electrophysiological recordings at the terminal site of the hippocampal medial perforant pathway primarily reflect the presynaptic Ca^{2+} currents and neurotransmitter release at presynaptic terminals of cortical spiny stellate neurons.

Selective Ca^{2+} channel subtype contributions to release at presynaptic terminals of the medial perforant path

Our Ca^{2+} imaging data indicate that Ca^{2+} current through P/Q-type channels contributes to ~50% of the total Ca^{2+} influx at perforant path presynaptic terminals. The ensuing release of neurotransmitter relies predominantly on P/Q-type channels, as indicated by a potent inhibition of synaptic transmission with the P/Q-type channel blocker ω-Aga IVA. This pattern is very similar to that found at the presynaptic terminals of hippocampal pyramidal neurons, cerebellar granule cells, and the calyx synapse in brainstem in several different species (Wu and Saggau, 1994b; Mintz et al., 1995; Wu et al., 1999). In contrast, Ca^{2+} current through N-type channels, although it contributes to ~30% of the total presynaptic Ca^{2+} entry and is comparable with the amount seen at hippocampal CA3–CA1 Shaffer collateral terminals (Qian and Noebels, 2000), has only a minor impact on neurotransmitter release at this synapse. By comparing the apparent power numbers for each type of Ca^{2+} channel (2.7 for P/Q and 0.4 for N), it can be concluded that the P/Q-type channel interacts more tightly with the release machinery than does the N-type channel at this synapse. A low power number for the N-type channel cannot be explained simply as the consequence of $[Ca_{pre}]_t$-dependent release, because reduction of $[Ca_{pre}]_t$ to ~75% of baseline by lowering $[Ca^{2+}]_o$ (to 1.5 mM) produced a greater power number. This preference of P/Q-type over N-type channels in the interaction with the release machinery has been observed at several central synapses (Mintz et al., 1995; Wu et al., 1999; Qian and Noebels, 2000) and may reflect the spatial arrangement of local channels near sites of neurotransmitter release (Bertram et al., 1999).

Elevated presynaptic Ca^{2+} influx at the release site ensures a high safety factor for synaptic transmission from entorhinal cortex to the hippocampus

Reliable quantal release of neurotransmitter with few failures has been found at synapses connecting stellate cells in layer IV of rat somatosensory cortex, in contrast to low release probability at the synaptic connection between layer V pyramidal cells (Feldmeyer et al., 1999; Feldmeyer and Sakmann, 2000). In this study, two lines of evidence point to a similar high release probability at the synapse from entorhinal cortex stellate cells to dentate granule cells when compared with hippocampal CA3–CA1 pyramidal neuron terminals. First, relatively smaller apparent power numbers in the Ca^{2+} cooperativity of neurotransmitter release were

measured compared with those obtained at the synapse between hippocampal pyramidal neurons of the same mouse strain (Qian and Noebels, 2000). This reduction in the apparent power number is apparently not attributable to a decreased Ca^{2+} cooperativity in the process of vesicle exocytosis, because the relationship between Ca^{2+} influx and neurotransmitter release can still be described by a fourth power function (Wu and Saggau, 1994a; Mintz et al., 1995; Borst and Sakmann, 1996). Rather, the smaller values indicate that the basal level of neurotransmitter release is closer to saturation levels at the presynaptic terminals of entorhinal cortical stellate cells than at those of hippocampal pyramidal cells. A small apparent power number when release approaches saturation is predicted by the Hill equation that describes the relationship between the optically measured Ca^{2+}influx and neurotransmitter release (Qian and Saggau, 1999). Second, the minor impact on neurotransmitter release observed after blocking N-type channels in normal $[Ca^{2+}]_o$ and the increased contribution of N-type channels to release in low $[Ca^{2+}]_o$ suggest that the release machinery is exposed to high Ca^{2+} entry under physiological conditions at this synapse. The contribution of N-type channels to neurotransmitter release only becomes evident when the degree in the overlap of Ca^{2+} microdomains is decreased. This is comparable with the observation made at the CA3–CA1 synapse, in which blocking N-type channels substantially inhibited neurotransmitter release under physiological conditions but had a much smaller effect on synaptic transmission when presynaptic Ca^{2+} entry was increased by broadening action potential duration (Wheeler et al., 1996; Qian and Saggau, 1999). Consequently, it is reasonable to conclude that the release machinery at this synapse is exposed to a larger Ca^{2+} influx than that present at the hippocampal CA3–CA1 synapse and that the synapse therefore exhibits a high release probability.

Potential molecular mechanisms underlying the different efficacies of cortical stellate neuron synapses and hippocampal pyramidal neuron synapses

Biophysical properties of voltage-gated Ca^{2+} channels are determined not only by the kinetics of the specific pore-forming α subunit but also by other ancillary interacting subunits, especially the β subunit (Walker and De Waard, 1998). Differential splicing and expression of α_{1A} subunits may account for the observed difference in efficacy between the cortical stellate neuron synapse and hippocampal pyramidal neuron synapse. The α_{1Ab} isoform is highly expressed in CA3–CA1 pyramidal neurons in the hippocampus (Bourinet et al., 1999). Although the α_{1A} subunit isoform expressed in the spiny neurons of entorhinal cortex is not yet known, study of neostriatal spiny neurons indicates that they exclusively express the α_{1Aa} isoform (Mermelstein et al., 1999). In the *Xenopus* oocyte expression system, the α_{1Ab} isoform displayed a significant 6 mV positive shift in the current–voltage relationship compared with that shown by the α_{1Aa} isoform (Bourinet et al., 1999). If layer II stellate cells in the entorhinal cortex also express α_{1Aa}, then P/Q-type Ca currents evoked by action potential invasion would be larger at the spiny neuron terminals than at the pyramidal neuron terminals, given an equal density of P/Q-type Ca^{2+} channels at both sites.

Alternatively, variability in the expression of ancillary Ca^{2+} channel subunits, especially the β subunit, provides another plausible mechanism for the difference observed between these two synapses. Single-cell reverse transcription-PCR analysis of Ca^{2+} channel α and β subunit mRNAs indicates different β subunit expression in neostriatal spiny stellate cells compared with cortical pyramidal cells (Mermelstein et al., 1999). Compared with cortical pyramidal cells, neostriatal spiny neurons express significantly higher levels of β_2 mRNA and lower levels of β_1 mRNA. Interestingly, this difference correlates well with the biophysical properties of Ca^{2+} Q-type channels in these two types of cell types. Q-type currents in the neostriatal spiny neurons display little or no inactivation. If entorhinal spiny neurons are similar to neostriatal spiny neurons and cortical pyramidal neurons are similar to hippocampal pyramidal neurons, presynaptic Q-type currents at the investigated synapse would be larger than those at the hippocampal CA3–CA1 synapse because they are less inactivated. To test whether the β_4 subunit is a potential candidate for this mechanism, we measured presynaptic Ca^{2+} channels and neurotransmitter release in lethargic mutants (*lh*), which lack functional β_4 subunits (Burgess et al., 1997). Similar to our previous findings at the hippocampal CA3–CA1 synapse (Qian and Noebels, 2000), presynaptic Ca^{2+} influx was comparable with wild type at the synaptic connection from entorhinal cortex to dentate gyrus in *lh* mice (data not shown). Thus, variable expression of β_4, if it exists in these two neurons, is unlikely to account for different properties of the presynaptic Ca^{2+} channels at these two synapses.

Finally, the possibility that a higher density of Ca^{2+} channels is present at the presynaptic terminals of stellate neurons in the layer II of entorhinal cortex than at those of hippocampal pyramidal neurons, although less likely, cannot be completely ruled out. Therefore, detailed study of Ca^{2+} channel subunit mRNA and the expressed proteins in these two cell types will be helpful in elucidating the basis for underlying differences in the biophysical properties of presynaptic Ca^{2+} channels at these two important synapses in the CNS.

REFERENCES

Alonso A, Klink R (1993) Differential electroresponsiveness of stellate and pyramidal-like cells of medial entorhinal cortex layer II. J Neurophysiol 70:128–143.

Bertram R, Simth GD, Sherman A (1999) Modeling study of the effects of overlapping Ca^{2+} microdomains on the neurotransmitter release. Biophys J 76:735–750.

Borst JGG, Sakmann B (1996) Calcium influx and transmitter release in a fast CNS synapse. Nature 383:431–434.

Bourinet E, Soong TW, Sutton K, Slaymaker S, Mathews E, Monteil A, Zamponi GW, Nargeot J, Snutch TP (1999) Splicing of alpha 1A subunit gene generates phenotypic variants of P- and Q-type calcium channels. Nat Neurosci 2:407–415.

Burgess DL, Jones JM, Meisler MH, Noebels JL (1997) Mutation of the Ca^{2+} channel beta subunit gene Cchb4 is associated with ataxia and seizures in the lethargic (lh) mouse. Cell 88:385–392.

Egger V, Feldmeyer D, Sakmann B (1999) Coincidence detection and changes of synaptic efficacy in spiny stellate neurons in rat barrel cortex. Nat Neurosci 2:1098–1105.

Feldman ML, Peters A (1978) The forms of non-pyramidal neurons in the visual cortex of the rat. J Comp Neurol 179:761–793.

Feldmeyer D, Sakmann B (2000) Synaptic efficacy and reliability of excitatory connections between the principal neurones of the input (layer 4) and output layer (layer 5) of the neocortex. J Physiol (Lond) 525:31–39.

Feldmeyer D, Egger V, Lubke J, Sakmann B (1999) Reliable synaptic connections between pairs of excitatory layer 4 neurones within a single "barrel" of developing rat somatosensory cortex. J Physiol (Lond) 521:169–190.

Klink R, Alonso A (1997) Morphological characteristics of layer II projection neurons in the rat medial entorhinal cortex. Hippocampus 7:571–583.

McNaughton BL (1980) Evidence for two physiologically distinct perforant pathways to the fascia dentata. Brain Res 199:1–19.

Mermelstein PG, Foehring RC, Tkatch T, Song WJ, Baranauskas G, Surmeier DJ (1999) Properties of Q-type calcium channels in neostriatal and cortical neurons are correlated with beta subunit expression. J Neurosci 19:7268–7277.

Mintz IM, Sabatini BL, Regehr WG (1995) Calcium control of transmitter release at a cerebellar synapse. Neuron 15:675–688.

Qian J, Noebels JL (2000) Presynaptic Ca^{2+} influx at a mouse central synapse with Ca^{2+} channel subunit mutations. J Neurosci 20:163–170.

Qian J, Saggau P (1999) Modulation of transmitter release by action potential duration at the hippocampal CA3–CA1 synapse. J Neurophysiol 81:288–298.

Qian J, Colmers WF, Saggau P (1997) Inhibition of synaptic transmission by neuropeptide Y in rat hippocampal area CA1: modulation of presynaptic Ca^{2+} entry. J Neurosci 17:8169–8177.

Steward O, Scoville SA (1976) Cells of origin of entorhinal cortical afferents to the hippocampus and fascia dentata of the rat. J Comp Neurol 169:347–370.

Walker D, De Waard M (1998) Subunit interaction sites in voltage-dependent Ca^{2+} channels: role in channel function. Trends Neurosci 21:148–154.

Wheeler DB, Randall A, Tsien RW (1994) Roles of N-type and Q-type Ca^{2+} channels in supporting hippocampal synaptic transmission. Science 264:107–111.

Wheeler DB, Randall A, Tsien RW (1996) Changes in action potential duration alter reliance of excitatory synaptic transmission on multiple types of Ca^{2+} channels in rat hippocampus. J Neurosci 16:2226–2237.

Woolsey TA, Dierker ML, Wann DF (1975) Mouse SmI cortex: qualitative and quantitative classification of golgi-impregnated barrel neurons. Proc Natl Acad Sci USA 72:2165–2169.

Wu LG, Saggau P (1994a) Presynaptic calcium is increased during normal synaptic transmission and paired-pulse facilitation, but not in long-term potentiation in area CA1 of hippocampus. J Neurosci 14:645–654.

Wu LG, Saggau P (1994b) Pharmacological identification of two types of presynaptic voltage-dependent calcium channels at CA3–CA1 synapses of the hippocampus. J Neurosci 14:5613–5622.

Wu LG, Westenbroek RE, Borst JGG, Catterall WA, Sakmann B (1999) Calcium channel types with distinct presynaptic localization couple differentially to transmitter release in single calyx-type synapses. J Neurosci 19:726–736.